CEBAF Program Advisory Committee Eight Cover Sheet

This proposal must be received by close of business on Thursday, April 14, 1994 at:

CEBAF
User Liaison Office, Mail Stop 12 B
12000 Jefferson Avenue
Newport News, VA 23606

Proposal Title

A MEASUREMENT OF t_{21} IN ELASTIC e-D SCATTERING

Contact Person

Name: JOE MITCHELL
Institution: CEBAF
Address: 12000 JEFFERSON AVE
Address: NEWPORT NEWS
City, State ZIP/Country: VA, 23606
Phone: (804) 249-7851 **FAX:** (804) 249-7363
E-Mail → Internet: MITCHELL@CEBAF.GOV

Experimental Hall:	HALL C
Total Days Requested for Approval:	20
Minimum and Maximum Beam Energies (GeV):	1.6
Minimum and Maximum Beam Currents (μAmps):	0.1

CEBAF Use Only

Receipt Date: 4/14/94 PR 94-013

By:

CEBAF PROPOSAL
A Measurement of t_{11} in Elastic e - D Scattering

R. Carlini, L. Cardman, R. Ent, D. Mack, J.H. Mitchell (spokesperson),
B. Vulcan, S. Wood, and C. Yan
Continuous Electron Beam Accelerator Facility
Newport News, VA, 23606

C. Cothran, D. Crabb, D. Day, R. Lindgren, R. Lourie,
J. S. McCarthy, P. McKee, R. Minehart, O. Rondon-Aramayo,
R. Sealock, C. Smith, and A. Tobias
Institute of Nuclear and Particle Physics
Department of Physics, University of Virginia
Charlottesville, VA 22901, USA

L. de Bever, A. Feltham, D. Fritschi, J. Jourdan,
M. Loppacher, S. Robinson and I. Sick
Institut für Physik, Universität Basel,
CH-4056, Basel, Schweiz

P. Ulmer
Department of Physics, Old Dominion University
Norfolk, VA, 23529

B. Wojtsekhowski
Department of Physics, Rensselaer Polytechnic Institute
Troy, N.Y. 12180

April 14, 1994

Abstract

We propose to measure the helicity asymmetry for the elastic scattering of polarized electrons from vector polarized deuterium. This will allow us to extract the vector response function, t_{11}, with high precision at $Q = 3.2$ fm^{-1} and at $Q = 3.8$ fm^{-1}. These data can be combined with existing measurements of A(Q) and B(Q) to separate the monopole and quadrupole form factors near the diffraction minimum of the former. This experiment will provide strong constraints on theoretical descriptions of the deuteron, in particular it addresses the role of isoscalar meson exchange contributions.

1 Introduction

The deuteron, being the simplest nucleus, has been the subject of intense experimental and theoretical examination. A detailed understanding of its structure provides insight into the nature of the nucleon-nucleon (NN) interaction [1]. The fact that it is a two body system allows *exact* theoretical calculations of the nucleonic aspects of its wave function.

The electromagnetic structure of the deuteron (spin 1) ground state is given by three form factors, here denoted, $G_M(Q)$ (monopole), $G_Q(Q)$ (quadrupole), and $G_D(Q)$ (magnetic dipole). In experiments with unpolarized electrons, unpolarized targets, and no measurement of the polarization of the recoiling deuteron, it is possible to separate two combinations of the three form factors. In order to separate all three form factors a polarization observable must be measured.

The cross section for the elastic scattering of unpolarized electrons from unpolarized deuterium is given by

$$\begin{aligned} \frac{d\sigma}{d\Omega} &= \sigma_{Mott} f_{rec}^{-1} F^2(Q,\theta_e) \\ F^2(Q,\theta_e) &= [A(Q) + B(Q)\tan^2\frac{\theta_e}{2}] \end{aligned}$$

where

$$\begin{aligned} \sigma_{Mott} &= \frac{\alpha^2 \cos^2\frac{\theta_e}{2}}{4E_e^2 \sin^4\frac{\theta_e}{2}} \\ f_{rec} &= 1 + \frac{2E_e \sin^2\frac{\theta_e}{2}}{M_d} \\ A(Q) &= G_M^2(Q) + \frac{2}{3}\eta G_D^2(Q) + \frac{8}{9}\eta^2 G_Q^2(Q) \\ B(Q) &= \frac{4}{3}\eta(1+\eta)G_D^2(Q) \\ \eta &= \frac{Q^2}{4M_d^2} \\ Q^2 &= -q_\mu^2. \end{aligned}$$

If a target with vector polarization, P_d, and tensor polarization, A_d, is used in conjunction with a beam of polarized electrons with polarization, p_e, the cross section takes the following form [2],[3]

$$\begin{aligned} \frac{d\sigma_{P_d,A_d,p_e}}{d\Omega} &= \Sigma + p_e\Delta \\ \Sigma &= \frac{d\sigma}{d\Omega}[1+\Gamma] \\ \Gamma &= A_d[\frac{1}{\sqrt{2}}P_2^0(\cos\theta^*)t_{20}(Q,\theta_e) + \frac{-1}{\sqrt{3}}P_2^1(\cos\theta^*)\cos\phi^* t_{21}(Q,\theta_e) \\ &+ \frac{1}{2\sqrt{3}}P_2^2(\cos\theta^*)\cos 2\phi^* t_{22}(Q,\theta_e)] \\ \Delta &= \frac{d\sigma}{d\Omega}P_d[\frac{\sqrt{3}}{\sqrt{2}}\cos\theta^* t_{10}(Q,\theta_e) - \sqrt{3}\sin\theta^*\cos\phi^* t_{11}(Q,\theta_e)]. \end{aligned}$$

where the notation has been chosen to make the connection with the Madison Convention clear [4]. The responses t_{ij} can be expressed in terms of the three form factors

$$
\begin{aligned}
t_{20}(Q,\theta_e)F^2(Q,\theta_e) &= \frac{-1}{\sqrt{2}}[\frac{8}{3}\eta G_M G_Q + \frac{8}{9}\eta^2 G_Q^2 + \frac{1}{3}\eta[1+2(1+\eta)\tan^2\frac{\theta_e}{2}]G_D^2] \\
t_{21}(Q,\theta_e)F^2(Q,\theta_e) &= \frac{2}{\sqrt{3}}\eta[\eta+\eta^2\sin^2\frac{\theta_e}{2}]^{\frac{1}{2}}\sec\frac{\theta_e}{2}G_D G_Q \\
t_{22}(Q,\theta_e)F^2(Q,\theta_e) &= \frac{-1}{2\sqrt{3}}\eta G_D^2 \\
t_{10}(Q,\theta_e)F^2(Q,\theta_e) &= \sqrt{\frac{3}{2}}\frac{2}{3}\eta[(1+\eta)[1+\eta\sin^2\frac{\theta_e}{2}]]^{\frac{1}{2}}\tan\frac{\theta_e}{2}\sec\frac{\theta_e}{2}G_D^2 \\
t_{11}(Q,\theta_e)F^2(Q,\theta_e) &= \frac{\sqrt{3}}{2}\frac{4}{3}[\eta(1+\eta)]^{\frac{1}{2}}\tan\frac{\theta_e}{2}G_D(G_M+\frac{1}{3}\eta G_Q).
\end{aligned}
$$

The angles θ^* and ϕ^* specify the quantization axis of the target with respect to the three momentum transfer, $\vec{q}$. $\theta^*=0$ when the target is polarized along $\vec{q}$ and $\phi^*=0$ or 180 in the electron scattering plane. The legendre polynomials multiplying the rank two responses are

$$
\begin{aligned}
P_2^0 &= \frac{1}{2}(3\cos^2\theta^*-1) \\
P_2^1 &= 3\cos\theta^*\sin\theta^* \\
P_2^2 &= 3\sin^2\theta^*.
\end{aligned}
$$

At $Q=0$ the normalizations of the form factors are given by the static properties of the deuteron

$$
\begin{aligned}
G_M(0) &= 1 \\
G_Q(0) &= M_d^2 Q_d = 25.83 \\
G_D(0) &= \frac{M_d}{M_p}\mu_d = 1.714.
\end{aligned}
$$

All the structure information is contained in the three quantities, $G_M(Q)$, $G_Q(Q)$ and $G_D(Q)$. In order to separate the three at a fixed value of Q it is necessary to measure three independent combinations of the form factors. Up to now this has been accomplished by combining the results of unpolarized Rosenbluth separations yielding A(Q) [5, 6, 7, 8] and B(Q) [9, 10, 11] with measurements of $t_{20}(Q,\theta_e)$ [12, 13, 14, 15, 16, 17]. The tensor response, t_{20}, can be measured by scattering unpolarized electrons from deuterium and then measuring the tensor polarization of the recoiling deuterons, or by scattering unpolarized electrons from a tensor polarized target. Both techniques have been utilized.

This preference for t_{20} as the third independent measurement has been largely due to the unavailability of high polarization electron beams. The term Γ containing t_{20} can be measured by exploiting the target- or recoil-alignment only. This term is independent of the electron helicity and hence does not require a polarized beam. Recently, the development of stressed gallium arsenide photo cathodes has enabled the preparation of low current (hundreds of nA) high polarization electron beams, $p_b \approx 80\%$. There have also been significant advances in the field of polarized deuterium targets. The Basel/UVA

collaboration has found that targets made from preradiated $^{15}ND_3$ dynamically polarized at 1 degree Kelvin in a 5 Tesla magnetic field yield very good deuteron vector polarizations, $P_d \approx 30$ to 35 %. This polarization can be maintained even in the presence of average electron currents of ≈ 100 nA. This represents a significant improvement in target figure of merit, $\propto I_{ave}P_d^2$. These technological developments make feasible a measurement of the vector response, t_{11}.

A measurement of t_{11} is attractive because, unlike recoil polarization, it requires no off–site calibration of a tensor (or vector) polarimeter. It also has an important advantage over polarized target measurements of t_{20} as t_{11} is proportional to a helicity asymmetry. Hence, t_{11} can be measured by simply flipping the electron beam polarization; such measurements are known to have very low systematic errors. In addition, one can further reduce possible systematic errors by reversing the target polarization (by changing the RF frequency).

t_{11} is attractive as compared to tensor polarization observables for a second reason: in experiments using solid targets it is impossible to flip the sign of the tensor polarization as $A_d = 2-\sqrt{(4-3P_d^2)} \geq 0$. Thus one must compare target polarized to target unpolarized measurements. While this does not preclude this type of measurement it does give only half the tensor asymmetry available from non-equilibrium targets such as atomic beam sources. The latter have their own special problems. For example it can be difficult to measure the tensor polarization in the target cell.

A measurement of t_{11} would give the same physics as measurements of the tensor polarization — complete separation of the three elastic form factors — but has much smaller systematic experimental errors.

2 Current Theoretical and Experimental Situation

The nonrelativistic impulse approximation, NRIA, with corrections for meson exchange currents, MECs, and isobar configurations, IC, has been extremely successful in predicting a variety of observables in the two and three nucleon systems. In the NRIA the virtual photon couples to the individual nucleons in the deuteron and the observed deuteron form factors are given by the isoscalar nucleon form factors and the deuteron S and D state wavefunctions. These wavefunctions are determined by the NN interaction. In this approach the structure of the monopole form factor, G_M, is dominated by the deuteron S-state wavefunction. In particular, the short-range repulsion in the NN interaction causes a node to appear in this form factor. The Q at which this node appears depends on the strength of the short-range repulsion. The presence of this node also affects t_{20} and t_{11} in the region of Q near the node.

MECs and other relativistic corrections, RC, have a tendency to move the node in G_M to lower values of Q and this shift is reflected in both t_{20} and t_{11}. Figures 1 - 3 show some recent calculations of the deuteron electromagnetic form factors in the NRIA with and without MECs [18]. The calculations shown utilize the Argonne V14 form of the NN interaction [19] and a dipole parameterization of the nucleon form factors. The MECs are treated in a manner consistent with the NN interaction (*ie.* current is conserved). The MECs include the "pair term" for both π and ρ exchange and the "true MECs", $\rho\pi\gamma$ and $\omega\pi\gamma$. In this region of momentum transfer the pion pair term is the dominant correction to both the monopole and magnetic form factors. The quadrupole form factor is little affected by these corrections. Other calculations combining NRIA with MEC's [20],[21] give similar results.

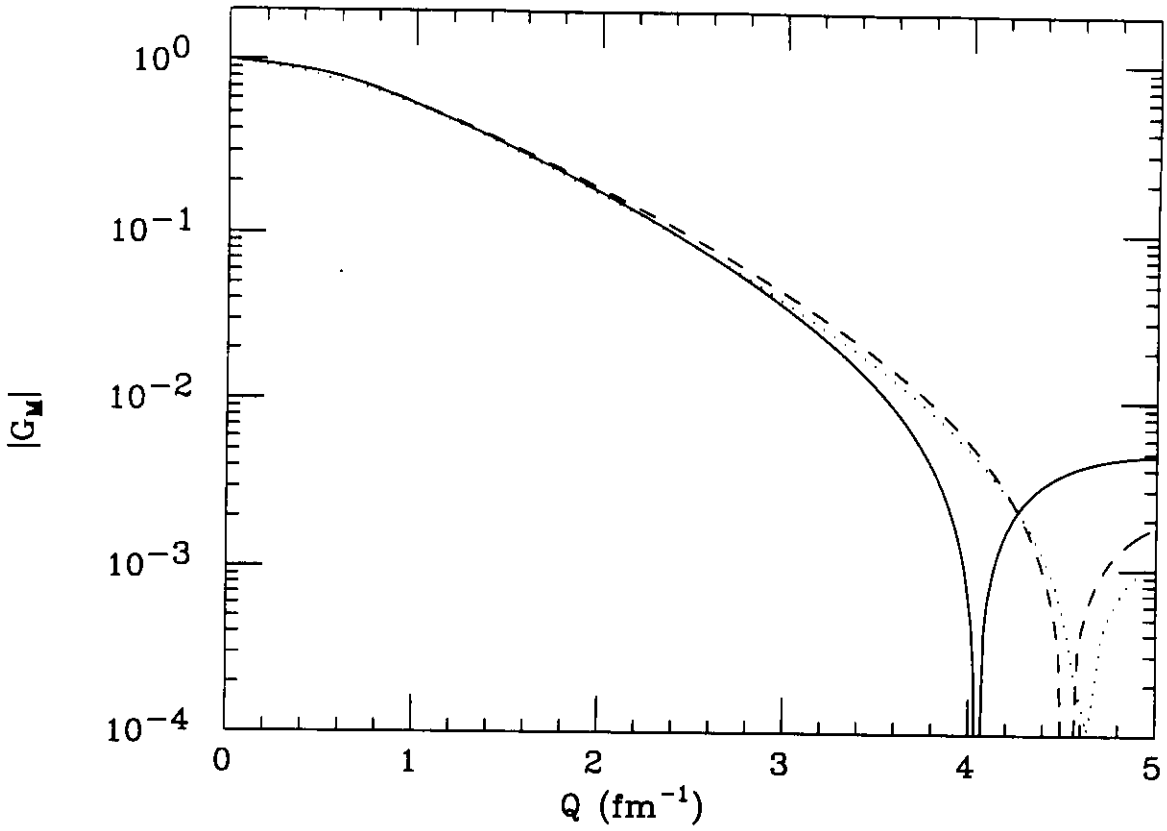

Figure 1: The monopole charge form factor, G_M, in various models, NRIA with MECs (solid), NRIA (dashes), and RIA with MECs (dots).

We have chosen the NRIA calculation described above, using dipole nucleon form factors, as the standard. In order to show the sensitivity of the observables to the physics included in the full calculation, we plot the percentage deviation from this calculation. In figures 4 and 5 calculations of the deviation of A(Q) and B(Q) are shown along with some experimental results [5],[10]. It is seen that even at these modest values of momentum transfer the data suggest that the corrections to the NRIA are important.

In figure 6 the predictions for t_{20} are shown. The calculations were performed at a constant beam energy of 1.6 GeV and the data were not corrected for the small angular effects. t_{20} is essentially independent of $G_D(Q)$ but is sensitive to corrections to the monopole charge form factor, $G_M(Q)$. The Bates data [14] favor the calculations which *omit* the MECs indicating that the node in G_M is at Q $\approx$ 4.4 fm^{-1} [15]. This is in conflict with results for the threshold electro-disintegration of the deuteron [18], the data for A(Q) [5], and the results for the monopole charge form factors of the other few nucleon systems, ^{3}H,^{3}He and ^{4}He [22, 23, 24]. Indeed, without the corrections to the charge density from pion exchange, the NRIA would consistently place the minima in the monopole charge form factors of light nuclei at too high a momentum transfer. It is worth noting that the dominating charge density correction in the three body nuclei is isoscalar in character and hence involves diagrams *identical* to the corrections that appear in the calculation of the deuteron monopole form factor. Figure 7 shows the measured

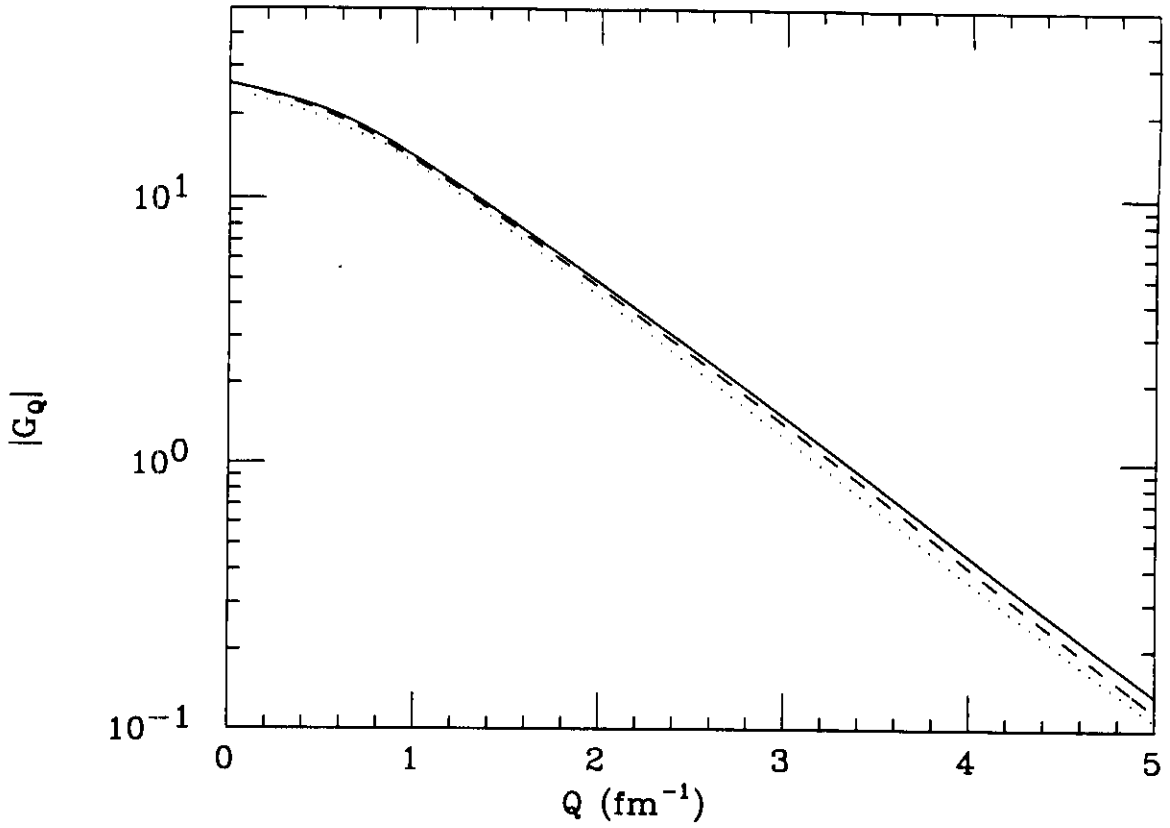

Figure 2: The quadrupole charge form factor, G_Q, in various models, NRIA with MECs (solid), NRIA (dashes), and RIA with MECs (dots).

isoscalar monopole form factor of the three nucleon system as well as calculations with and without MEC's [25, 22, 24]. The MECs clearly are needed in order to describe these data.

The deuteron monopole form factor thus stands apart, and represents a major anomaly.

We note that the latest t_{20} data from Novosibirsk [17], while of low statistics, are in conflict with the recoil measurements from MIT Bates [14].

The NRIA with MECs also provides a consistent picture of the magnetic structure of light systems [26],[27]. The current density corrections from MECs are needed in order to obtain agreement with the measured magnetic form factors of these nuclei. In fact, the current density corrections which enter in the case of the magnetic form factors are on even firmer theoretical footing than are the charge density corrections responsible for the shifts in the monopole form factors [22].

For the deuteron there are also relativistic calculations available. Tjon and co-workers have solved the Bethe-Salpeter equation in the ladder approximation using a meson exchange driving force [28, 29]. In this formalism the pair term is implicitly included and one need only add the "true MECs", $\rho\pi\gamma$ and $\omega\pi\gamma$ [30, 31]. They find that the exchange type corrections to the isoscalar part of the electromagnetic current are small and hence their calculations tend to be very similar to the NRIA without any corrections. The small effect of the pion exchange in their calculations is evidently due to a cancellation

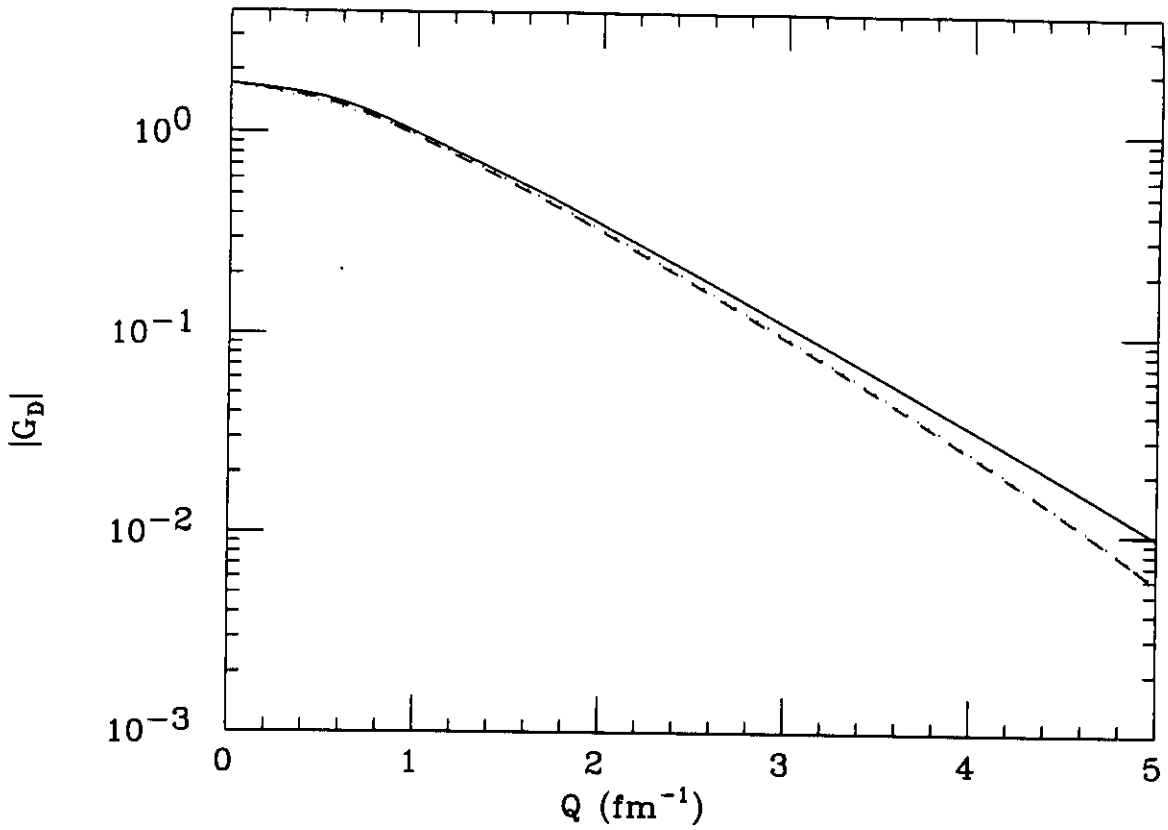

Figure 3: The magnetic dipole form factor, G_D, in various models, NRIA with MECs (solid), NRIA (dashes), and RIA with MECs (dots).

[32]. The use of pseudo-scalar coupling for the pion leads to a cancellation between one and two pion exchange contributions that is responsible [29] for the small effect (most of their calculations including the ones shown in this document use pseudo-vector coupling for the pion). These relativistic calculations have been included in figures 4, 5 and 6. The data for t_{20} are in good agreement with the calculations employing this approach. However, the reproduction of A(Q) and B(Q) is much less good than that of the full non-relativistic calculation.

Overall, this situation is very unsatisfactory. It leaves us with an important discrepancy between the otherwise successful NRIA+MEC calculations and the data. It also leaves unresolved the question of consistency with the charge and magnetic form factors of the three body nuclei and the monopole charge form factor of ^{4}He.

The experiment proposed here intends to *focus* on the monopole form factor in the region of the minimum, and provide an *independent* measurement with low systematic errors.

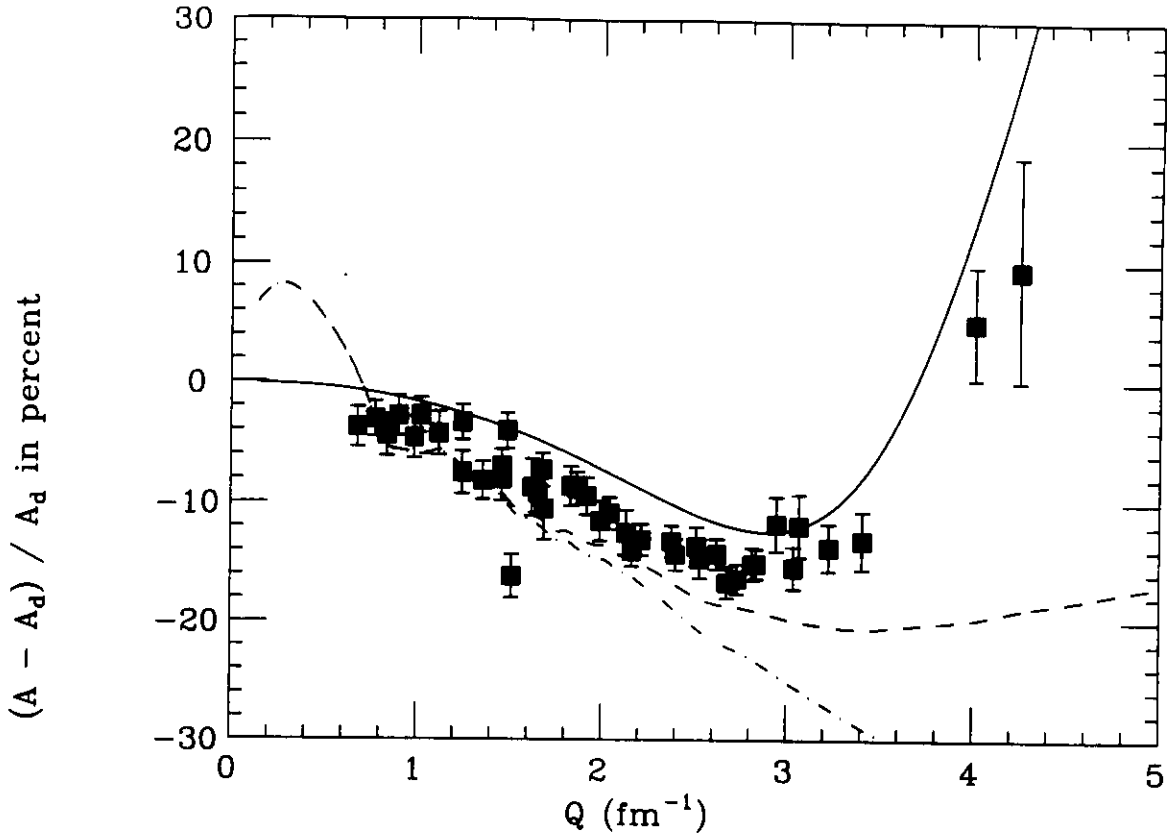

Figure 4: The percent deviation from the NRIA with dipole parameterization of the nucleon form factors of A(Q). The data are from [5]. The curves are calculations from various models, NRIA with MECs (solid), RIA (dash-dot), RIA with MECs (dashes).

3 The Proposed Experiment

The proposed experiment plans to measure $\vec{d}(\vec{e}, e)d$ using a polarized deuterium target and a polarized beam, detecting the scattered electron using the HMS spectrometer and detecting the recoil deuteron in a ΔE/E plastic array for identification of the deuterons.

We plan to measure the helicity asymmetry in elastic electron scattering from polarized deuterons in a dynamically polarized $^{15}ND_3$ target at two values of the four momentum transfer, Q = 3.2 fm^{-1} and Q = 3.8 fm^{-1}. The target will be polarized in the electron scattering plane perpendicular to the momentum transfer, $\vec{q}$. This will allow us to extract the vector response, t_{11}, with small statistical and systematic uncertainties. Figure 8 shows theoretical predictions for t_{11} at a constant beam energy of 1.6 GeV. t_{11} is a product of G_D and a linear combination of G_M and G_Q. G_D is extracted from measurements of B(Q) and is known to about 5 % at intermediate Q [10]. For the presentation in this proposal we exploit the fact that the NRIA with MEC's provides a reasonable description of B(Q) (see figure 5); we thus will consider it as a 'fit' to the data and use it for the magnetic contribution to t_{11} in both nonrelativistic calculations. Curves are shown for several models of the monopole form factors; NRIA, NRIA + MECs and the full calculation of Tjon and collaborators. This shows that t_{11} can provide a good

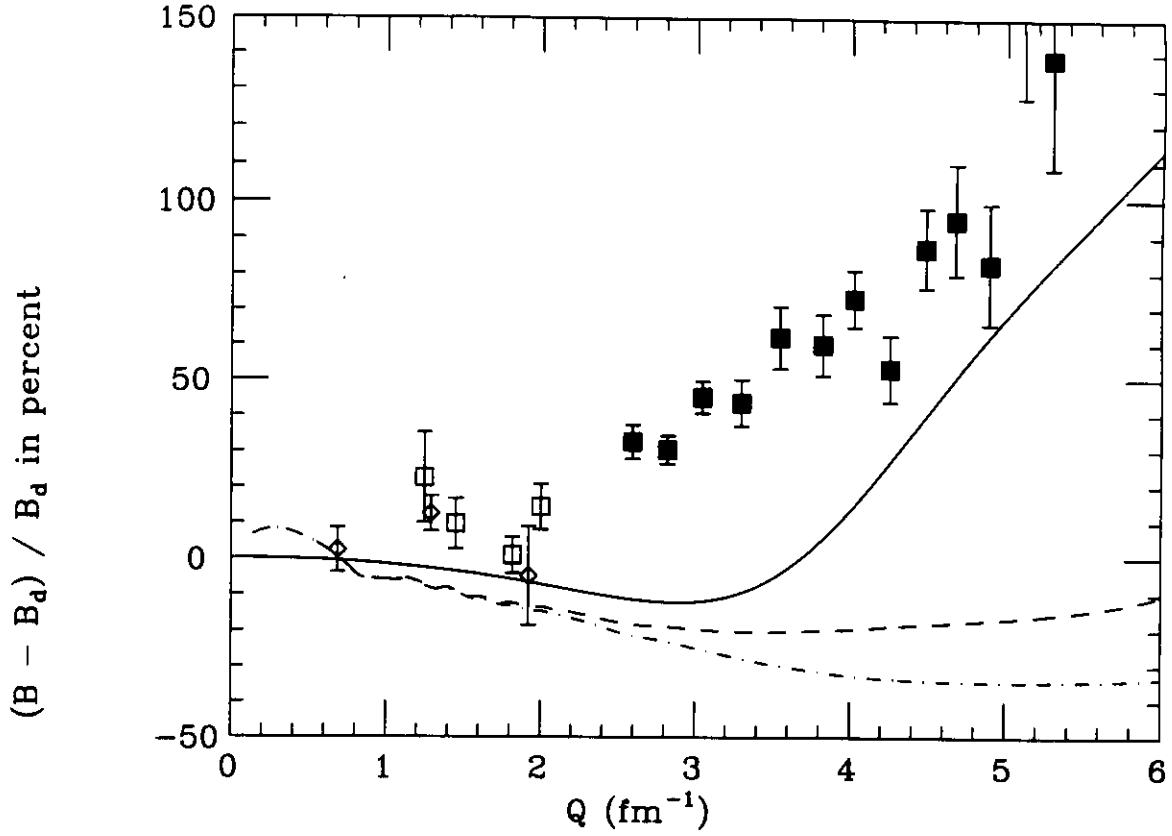

Figure 5: The percent deviation from the NRIA with dipole parameterization of the nucleon form factors of B(Q). The data are from [10]. The curves are calculations from various models, NRIA with MECs (solid), RIA (dash-dot), RIA with MECs (dashes).

measure of the charge corrections to the NRIA. The data points shown in the figure show the error bars that would be obtained in the proposed Hall C measurement.

The experiment requires a highly polarized low current electron beam such as that produced by a laser-driven source with a stressed gallium arsenide photo cathode as employed at SLAC during the recent measurements of the neutron and proton polarized deep inelastic structure functions (SLAC experiment E143)[33]. During E143, beam polarizations of 85 % were routinely obtained. An approved experiment in Hall C to measure the neutron's electric form factor, G_{en}, has similar requirements, so this experiment places no new demands in this area [34]. The beam polarization will be monitored periodically by measuring the asymmetry in Moller scattering with the Hall-C Moller polarimeter which is being built by members of this collaboration.

The polarized target is the same target as that used by the Basel/UVA collaboration for E143 and built for use in the CEBAF measurements of G_{en} and the deformation of the nucleon [35]. During E143, deuteron polarizations of up to 40 % were obtained and the target was operated with average beam currents approaching 100 nA. Table 1 summarizes the target thickness assumed in the count rate and run time estimates. The target thickness quoted corresponds to 2 cm of $^{15}ND_3$ with a density of 0.9 and a packing fraction of the ammonia beads of 0.55. The luminosities correspond to 90 nA of beam

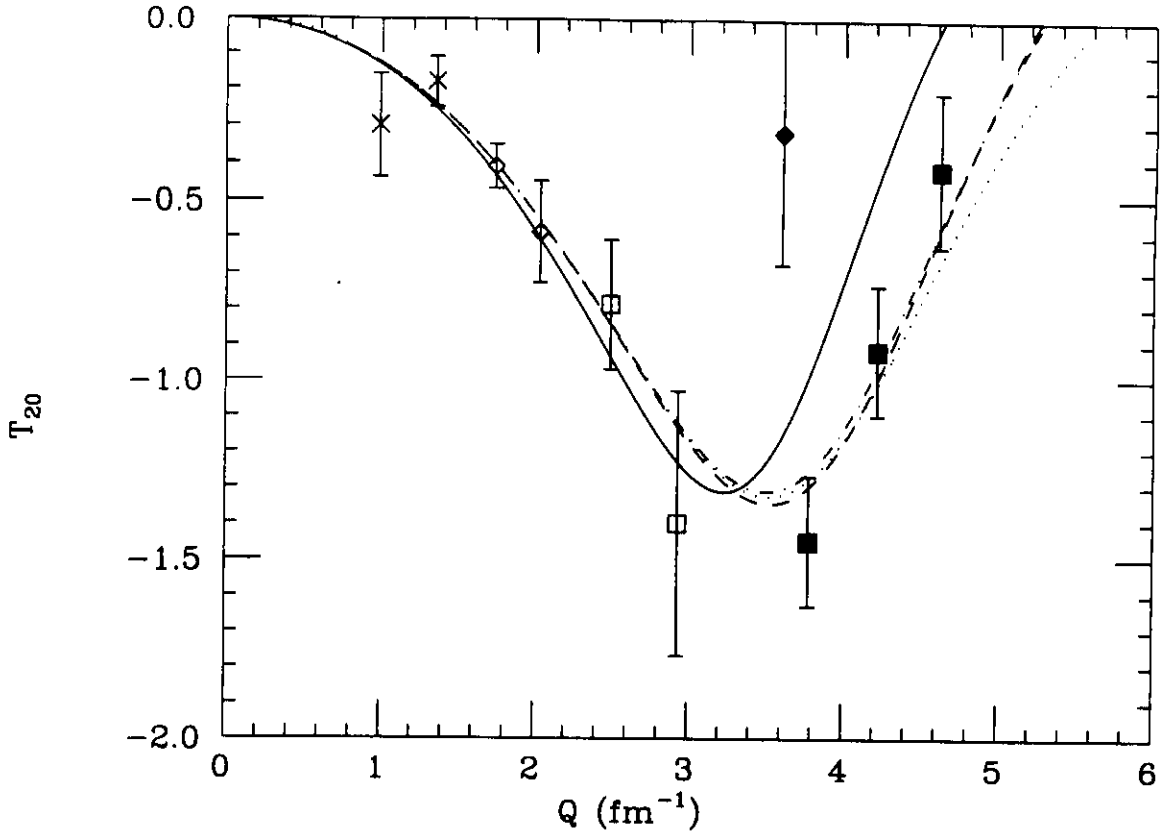

Figure 6: The results of various tensor polarization measurements taken from [15] and theoretical predictions. The solid curve is the NRIA with MECs, dashed curve is NRIA, dots RIA, dot-dash RIA + MECs.

and we have assumed 80 percent for the beam polarization. The nitrogen and helium luminosities are those used for calculating background rates. We expect no appreciable dilution as we will have good proton - deuteron discrimination and good missing energy resolution to suppress quasi elastic knockout of deuterons from nitrogen and helium.

The elastically scattered electrons will be detected in the HMS spectrometer in its large solid angle tune, $d\Omega \approx 10$msr.

Table 2 gives the kinematic quantities for the proposed measurements. A beam energy of 1.6 GeV is requested.

Table 3 shows the magnitude of the deflections suffered by the charge particles as they traverse the target field. Φ_e ($\Phi_{e'}$) is the vertical deflection of the incoming (scattered) electrons and Φ_d is the deflection of the recoiling deuterons. These values were obtained by a numerical integration of the equations of motion in the calculated field map of the target magnet. This field map is a theoretical map supplied by the magnet's manufacturer, Oxford Instruments. The angle θ_B specifies the orientation of the target holding field with respect to the beam line. The deflection of the incoming and unscattered electron beam will be compensated by a series of chicane magnets which are presently being installed in the hall C beam line.

The recoiling deuterons will be detected in an array of plastic scintillators. Deuteron

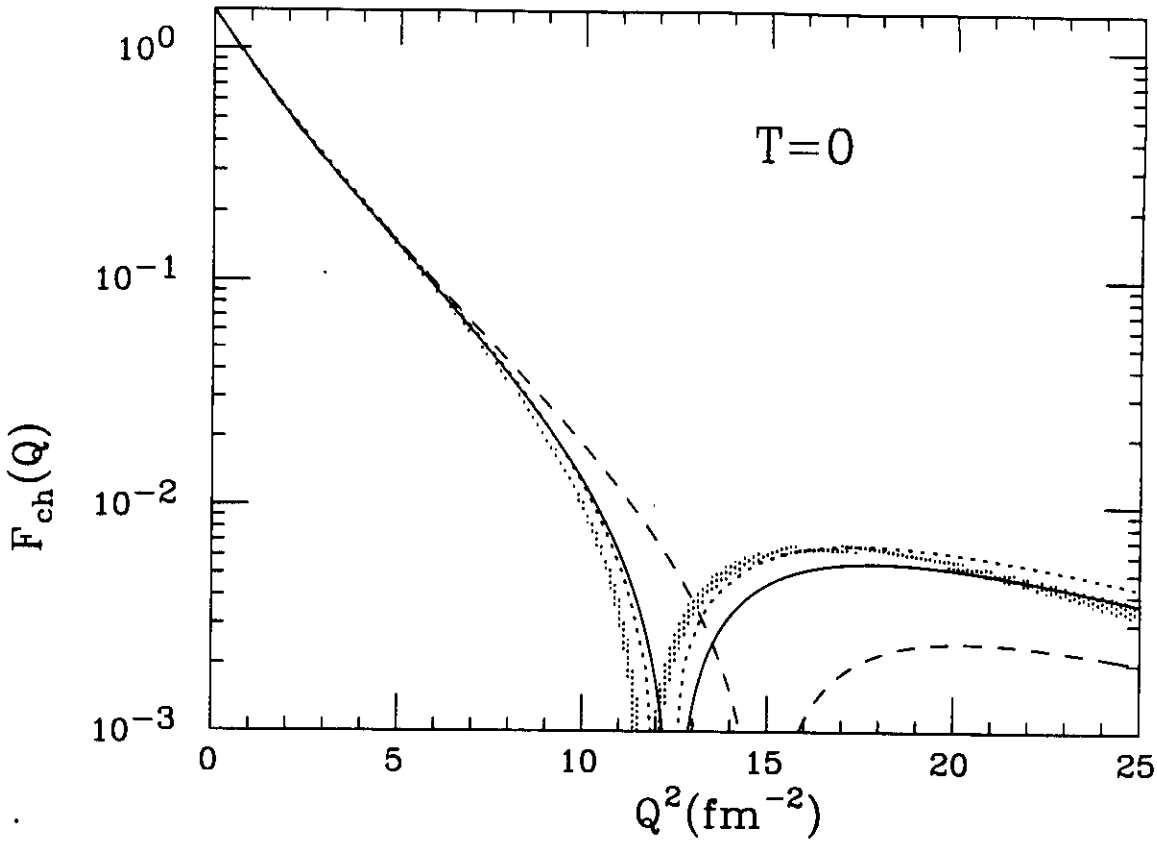

Figure 7: The isoscalar charge form factor of the three-body nuclei. The solid curve is the NRIA with MECs calculation of reference [24], the long dash is the NRIA calculation of the same group and the short dash curve is the NRIA with MECs of reference [22]. The error band is a recent fit to the data for elastic electron scattering from ^{3}H and ^{3}He [25].

identification will be accomplished by three methods, ΔE vs E, time of flight, and kinematic correlation.

The angular coverage that is required for the deuteron detector array to match the acceptance of the HMS in the 10 msr tune was determined by monte carlo simulations using the code MCEEP [36]. The array must cover $\pm$ 12.5 deg in the vertical angle and must subtend 3.5 deg in the horizontal plane. Plastic scintillators 1.6 meters long placed at 2.75 meters from the target center provide angular coverage of $\pm$ 16.2 deg which is adequate even after including the effects of multiple scattering in the target material. The lowest energy deuterons are expected to have RMS planar multiple scattering angles of about 0.7 deg.

The dominate coincident background is expected to be from quasi elastic proton knockout. The coincident proton rates from $^{15}N(e,e'p)$ and $^4He(e,e'p)$ are shown in table 4 along with the rates for the elastic scattering, $\vec{D}(e,e'd)$. The coincident proton rates were determined by monte carlo simulations with MCEEP. We estimate that the quasi elastic $(e,e'd)$ rates from nitrogen and helium are 25 to 30 % of the elastic rate. This is based on the results from the Bonn t_{20} measurement [16] and from high resolution

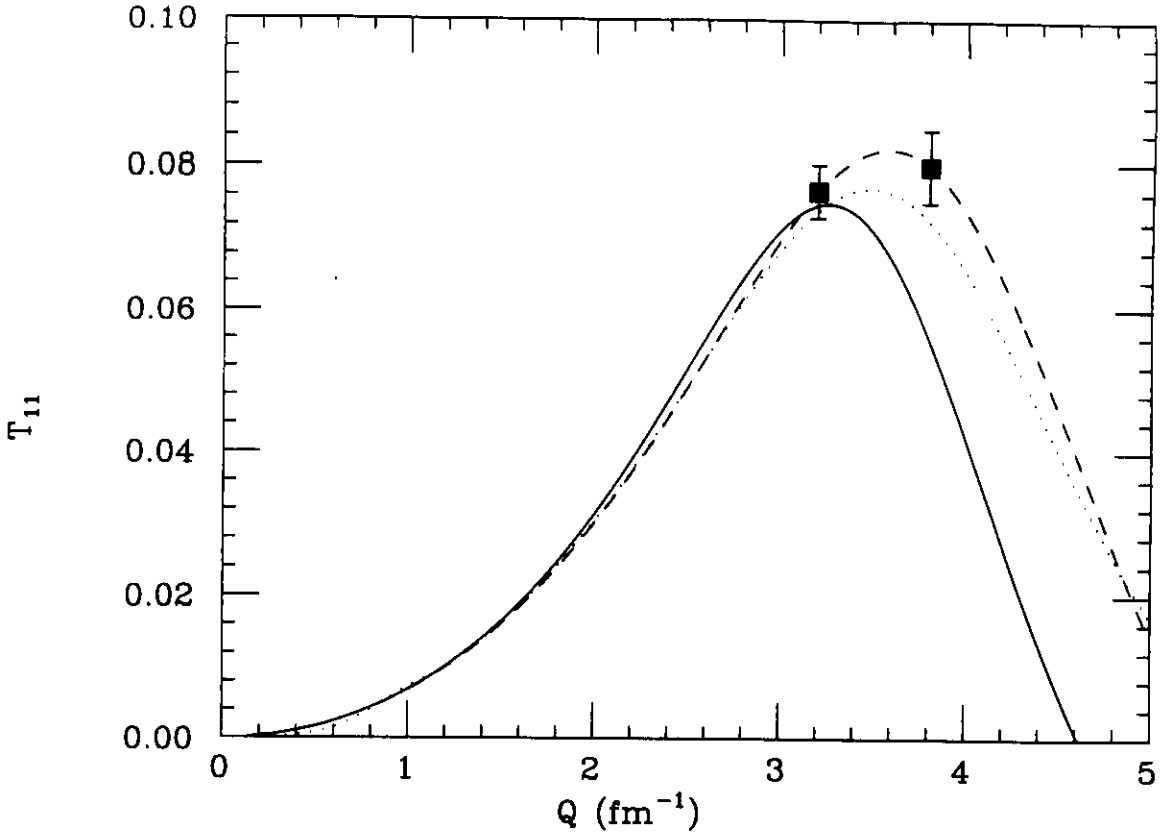

Figure 8: Model predictions for the vector polarization, t_{11}. Solid curve is NRIA + MECs, dash NRIA with realistic magnetic contribution, dots RIA with MECs. The data points are the anticipated results from the proposed measurement.

measurements of $^{12}C(e,e'd)$ and $^{4}He(e,e'd)$ performed at NIKHEF-K [37],[38]. The entry labeled $(e,e'p)$ is just the sum of the nitrogen and helium $(e,e'p)$ rates. The entry labeled 'angle cut' is the $(e,e'p)$ rate after cutting on the elastic peak in the electron arm and making a 2° cut on the angle between $\vec{q}$ and the momentum vector of the detected hadron. To determine this angle to 2 degrees requires a 10% knowledge of the field integral and a position resolution at 2.75 meters of about 10 cm. The calculated field maps are close to this level of accuracy but can be checked by looking at $H(e,e'p)$ from a NH_3 target. The 10 cm resolution in the plastic scintillators is straightforward to obtain. This angle cut will also suppress some quasi elastic deuterons.

Deuterons in the energy range of interest have about 1.7 times greater dE/dx than protons. They also suffer about a 20 % pulse height deficit compared to protons of the same energy. This means that deuterons give about 35 percent more light in plastic scintillator than protons of the same energy. This is a very favorable energy range for ΔE vs E deuteron - proton discrimination. The deuterons of interest have ranges varying from about 3.8 to 8.5 cm of plastic. Thus we will use an array of 1 cm ΔE paddles backed by 10 cm thick E detectors for particle identification throughout the entire energy range. A suitable detector can be assembled using elements of the plastic scintillator array that will be used in the G_{en} experiment.

Nucleus	$\vec{P}_d$%	A_d%	L ($cm^{-2}sec^{-1}$)
D	35	9.4	9.1 10^{34}
^{15}N	$\approx$ 18	0	2.2 10^{34}
^{4}He	0	0	1.2 10^{34}

Table 1: Target characteristics used in count rate, run time and background rates estimates.

Q (fm^{-1})	E' (GeV)	θ_e	θ_d	T_d (MeV)
3.2	1.493	23.6	-68.8	107.0
3.8	1.45	28.5	-64.8	150.0

Table 2: Kinematics for t_{11} measurement at E_e = 1.6 GeV.

The target cell will have 1 cm (horizontal) and 2 cm (vertical) dimensions transverse to the beam direction. The beam will be rastered at about 10 Hz over the face of the cell and the beam position on the face will be recorded in the data stream so that target path length corrections can be made for the outgoing charged particles. Typical deuterons lose less than 10 MeV in the target windows and material, hence the detector resolution should not be significantly degraded.

At 2.75 meters a timing resolution of 1 ns with a path length uncertainty of 5 cm would give a missing energy resolution of 15 MeV (for the highest energy deuterons). Even this modest resolution would essentially eliminate the background due to quasi elastic knockout of deuterons from nitrogen (E_m = 16.8 MeV) and helium (E_m = 23.8 MeV). Note that the 1 cm thick scintillators of the detector have mean time resolutions of order 100 ps for minimum ionizing particles. Missing mass reconstruction via time of flight will also suppress the proton background.

In the Bonn t_{20} measurement [16], which was performed with a similar target, a background separation using time of flight vs momentum (they had a crude magnetic spectrometer for the deuterons) was quite good. They also used the kinematic correlation for separating the elastic events from the quasi elastic background. We feel that we can do at least as good and probably much better as they did not use ΔE vs E. The beam time request includes a 10% dilution of the polarization due to background from processes other than d(e,e)d, and time for measuring backgrounds by looking for deuteron

Q (fm^{-1})	Φ_e	$\Phi_{e'}$	Φ_d	θ_B
3.2	2.8	0.3	16.2	21.2
3.8	3.3	0.5	10.9	25.2

Table 3: Particle deflection angles in degrees due to the target holding field for E_e = 1.6 GeV.

coincidences from a $^{15}NH_3$ target. The singles rates in the plastic scintillators are low due to the relatively low luminosity, large deuteron scattering angle, and the fact that the 5 Tesla holding field of the target sweeps away the low energy charged particles.

Reaction	Q (fm^{-1})	R (Hz)
$\vec{D}(e,e'd)$	3.2	1.8
$\vec{D}(e,e'd)$	3.8	0.23
$^{15}N(e,e'p)$	3.2	41
$^{15}N(e,e'p)$	3.8	12
$^{4}He(e,e'p)$	3.2	5.0
$^{4}He(e,e'p)$	3.8	1.2
(e,e'p)	3.2	46.0
(e,e'p)	3.8	13.2
angle cut	3.2	0.32
angle cut	3.8	0.25

Table 4: Rates in Hz for elastic scattering and proton knockout.

4 Beam time request

The target will be polarized in the scattering plane and perpendicular to the momentum transfer ($\phi^* = 0$ and $\theta^* = 90$ deg). The helicity asymmetry is then

$$A_h = -p_e P_d df \sqrt{3} t_{11}.$$

where p_e and P_d are the beam polarizations of the beam and target and df is the dilution factor (taken to be 0.9). The required run time for a measurement of t_{11} with a fractional statistical uncertainty of $\epsilon = \Delta A_h / A_h$ can be calculated from

$$t_{beam}(hours) = \frac{1}{(\epsilon A_h)^2 R(Hz) \gamma 3600}$$

where R(Hz) is the elastic scattering rate in Hertz, the 3600 is for unit conversion, and γ corrects for radiative loses (taken to be 0.8). The expected helicity asymmetries are of order a few percent. The requested beam times estimated from the NRIA with a realistic magnetic contribution are given in table 5. The table also includes the time required for annealing the target, making thermal equilibrium NMR calibration measurements, and making Moller beam polarization measurements. The time required for the installation and removal of the polarized target and the detector array is not included in the table. The impact of this experiment on scheduling can be minimized by running it in series with the other polarized target experiments in Hall C.

The systematic uncertainties in the experiment are largely due to ones ability to determine the polarization of the beam and the target. Moller polarimetry can give the beam polarization with a systematic uncertainty between 1 and 3 % and NMR

target	Q (fm^{-1})	A_h%	ϵ%	t_{beam} (hours)
ND_3	3.2	3.3	5	70
ND_3	3.8	3.5	6.7	280
NH_3	3.2			7
NH_3	3.8			28
Moller				32
Anneals				20
Thermals				16
Overhead				35
Total				488

Table 5: Requested run times, expected asymmetries and statistical uncertainties for the proposed measurement of t_{11}. The measurements at both momentum transfers require 1.6 GeV polarized beam.

measurements can give the deuteron polarization with an uncertainty of about 4 %. Adding these errors in quadrature the overall systematic is less than 5 %.

t_{11} is itself sensitive to the physics we wish to investigate, the position of the node in G_M, but by combining the polarization data with measurements of A and B at the same momentum transfer it is possible to separate G_M and G_Q. Figure 9 shows the anticipated error bars for G_M that would be obtained by combining the results of a Hall C measurement of t_{11} with the Saclay data for A(Q) [5] and B(Q) [10]. The error bars include the effects of systematic and statistical errors in each of the observables. Error bars are shown for both positions of the minimum. The figure also includes the results of a complete form factor separation based on the world's t_{20} data [15]. The errors in the extracted quadrupole form factor would be similar in magnitude.

5 Summary

A consistent picture of the few body nuclei is needed if we are to claim any real understanding of nuclear dynamics. Unpolarized electron scattering data from all few body systems seem to decisively indicate the need for inclusion of MEC corrections to the NRIA. However, recent data obtained for t_{20} for e–d scattering seem to indicate that these corrections are *not needed* in this observable. Precision measurements of the elastic vector response, t_{11}, will provide an important complementary measurement of the deuteron electromagnetic form factors. These data will have smaller systematic uncertainties than are available from recoil polarization measurements. In a region of momentum transfer where there is great sensitivity to the position of the node in the Monopole form factor, it is possible to get good statistical precision in a relatively modest amount of beam time, and no extra effort on the hardware side.

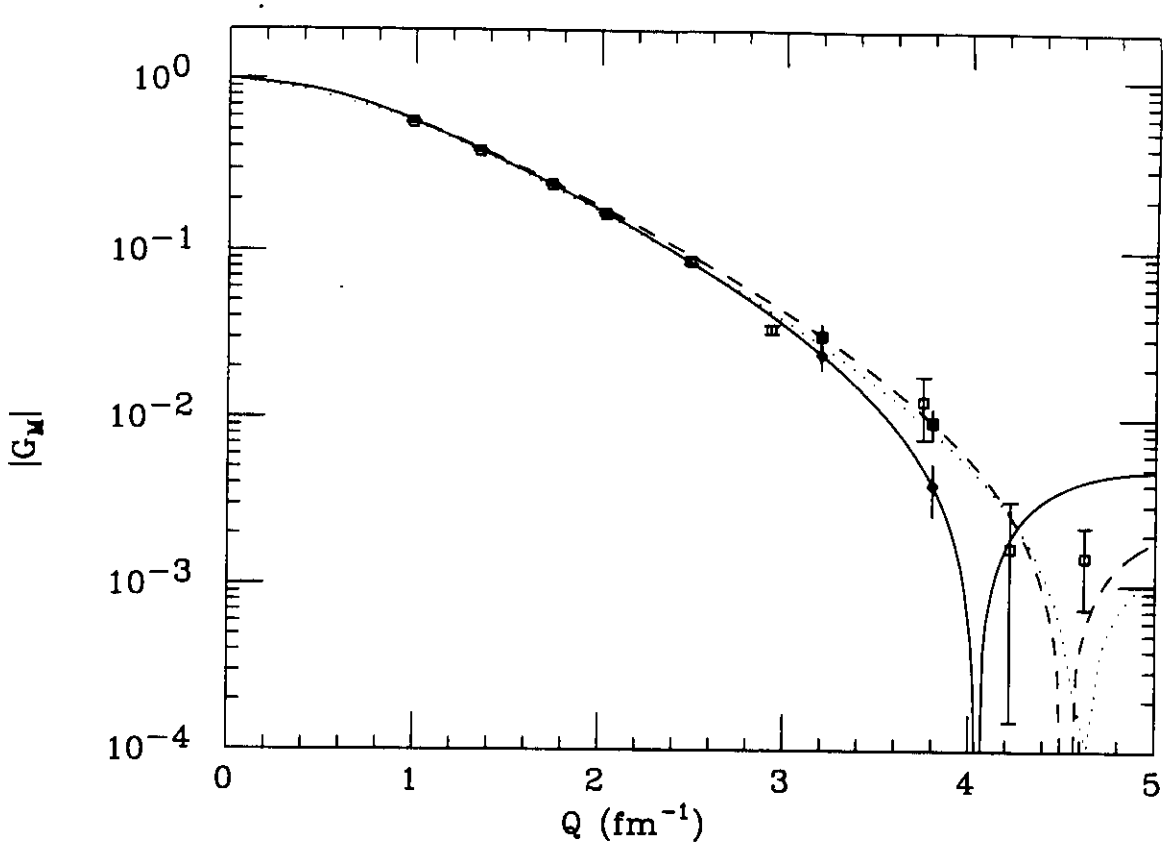

Figure 9: G_M from the form factor separation of reference [15] (open points). Also shown are the anticipated results from a combination of the proposed measurement with existing data for A(Q) and B(Q) (solid points). The solid squares are for NRIA position of the minimum, while the solid triangles are for the NRIA + MECs position of the minimum. The curves are the same as figure 1.

References

[1] E.L. Lomon, Annals of Phys. **125**, 309 (1980)

[2] T.W. Donnelly and A.S. Raskin, Annals of Phys. **169** 247 (1986)

[3] R.G. Arnold, C.E. Carlson, and F. Gross, Phys. Rev. **C23** 363 (1981)

[4] S.E. Darden, "Polarization Phenomena in Nuclear Reactions", (edited by Barschall and Haberli) pg 39 Univ. of Wisconsin Press (1970)

[5] S. Platchkov *et al.*, Nucl. Phys. **A508**, 445 (1990)

[6] G.G. Simon, Ch. Schmitt, and V.H. Walther, Nucl. Phys. **A364**, 285 (1981)

[7] R.G. Arnold *et al.*, Phys. Rev. Lett. **35**, 776 (1975)

[8] J.E. Elias *et al.*, Phys. Rev. **177**, 2075 (1969)

[9] P.E. Bosted *et al.*, Phys. Rev. **C42**, 38 (1990)

[10] S. Auffret *et al.*, Phys. Rev. Lett. **54**, 649 (1985)

[11] R. Kramer *et al.*, Z. Phys. **Z 29**, 513 (1985)

[12] B.B. Voitsekhovskii *et al.*, JEPT Lett. **43**, 733 (1986)

[13] R. Gilman, *et al.*, Phys. Rev. Lett. **65**, 1733 (1990)

[14] I. The, *et al.*, Phys. Rev. Lett. **67**, 173 (1991)

[15] M. Garçon, *et al.*, to be published.

[16] B. Boden *et al.*, Z. Phys. **C49**, 175 (1991)

[17] Novosibirsk (1992) unpublished.

[18] R. Schiavilla and D.O. Riska, Phys. Rev. **C43**, 437 (1990)

[19] R.B. Wiringa, R.A. Smith, and T.L. Ainsworth, Phys. Rev. **C29**, 1207 (1984)

[20] M.I. Haftel, L. Mathelitsch, and H.F.K. Zingl, Phys. Rev. **C22**, 1285 (1980)

[21] M. Gari and H. Hyuga, Nucl. Phys. **A264**, 409 (1976)

[22] R. Schiavilla, V.R. Pandharipande, and D.O. Riska, Phys. Rev. **C41**, 309 (1990)

[23] W.M. Kloet and J.A. Tjon, Phys. Lett. **49B**, 419 (1974)

[24] W. Struve, *et al.*, Nucl. Phys. **A465**, 651 (1987)

[25] I. Sick, private communication.

[26] R. Schiavilla, and D.O. Riska, Phys. Lett. **244B**, 373 (1990)

[27] R. Schiavilla, V.R. Pandharipande, and D.O. Riska, Phys. Rev. **C40**, 2294 (1989)

[28] M.J. Zuilhof and J.A. Tjon, Phys. Rev. **C22**, 2369 (1980)

[29] M.J. Zuilhof and J.A. Tjon, Phys. Rev. **C24**, 736 (1981)

[30] E. Hummel and J.A. Tjon, Phys. Rev. Lett. **63**, 1788, (1989)

[31] E. Hummel and J.A. Tjon, Phys. Rev. **C42**, 423, (1990)

[32] J.A. Tjon and M.J. Zuilhof, Phys. Lett. **84B**, 31 (1979)

[33] O. Rondon-Aramayo and R. Arnold co-spokesmen, " Measurements of the Nucleon Spin Structure Functions at SLAC in End Station A ", data acquisition completed in Dec. 1993

[34] D. Day spokesperson, "The Charge Form Factor of the Neutron", CEBAF Proposal PR-93-026, approved for 60 days in Hall C.

[35] J. Jourdan spokesperson, "Deformation of the Nucleon", CEBAF Proposal PR-93-028, approved for 15 days in Hall C.

[36] P.E. Ulmer, "**MCEEP**: Monte Carlo for Electro-Nuclear Coincidence Experiments", CEBAF Technical Note 91-101 (1991)

[37] R. Ent *et al.*, Phys. Rev. Lett. **62**, 24 (1989)

[38] R. Ent *et al.*, Phys. Rev. Lett. **67**, 18 (1991)

HAZARD IDENTIFICATION CHECKLIST

A MEASUREMENT OF $\vec{t}_{11}$ IN ELASTIC e-D SCATTERING

CEBAF Experiment: _____ Date: 4/14/93

Check all items for which there is an anticipated need—do not check items that are part of the CEBAF standard experiment (HRSE, HRSH, CLAS, HMS, SOS in standa configurations).

Cryogenics
- ____ beamline magnets
- ____ analysis magnets
- ✓ target
- ____ drift chambers
- ____ other

Electrical Equipment
- ____ cryo/electrical devices
- ____ capacitor banks
- ____ high voltage
- ____ exposed equipment

Radioactive/Hazardous Materials
List any radioactive or hazadorous/ toxic materials planned for use:
_____
_____

Pressure Vessels
- ____ inside diameter
- ____ operating pressure
- ____ window material
- ____ window thickness

Flammable Gas or Liquids
(incl. target)
type: _____
flow rate: _____
capacity: _____

Other Target Materials
- ___ Beryllium (Be)
- ___ Lithium (Li)
- ___ Mercury (Hg)
- ___ Lead (Pb)
- ___ Tungsten (W)
- ___ Uranium (U)
- ✓ Other (list below)

NH_3, ND_3

Vacuum Vessels
- ~1 METER inside diameter
- ____ operating pressure
- ____ window material
- ____ window thickness

Radioactive Sources
- ____ permanent installation
- ____ temporary use

type: _____
strength: _____

Large Mech. Structure/System
- ____ lifting devices
- ____ motion controllers
- ✓ scaffolding or elevated platforms
- ____ other

Lasers
type: _____
wattage: _____
class: _____

Installation
- ____ permanent
- ____ temporary

Use
- ____ calibration
- ____ alignment

Hazardous Materials
- ___ cyanide plating materials
- ___ scintillation oil (from)
- ___ PCBs
- ___ methane
- ___ TMAE
- ___ TEA
- ___ photographic developers
- ___ other (list below)

_____
_____
_____

Notes:

EXPERIMENT REQUIRES A POLARIZED TARGET. A PLATFORM IS NEEDED FOR THE TARGET SYSTEM E.G. FOIL AN ARRAY OF PLASTIC SCINTILLATORS